

1 **Supporting Material to Neural network-based estimates of Southern Ocean**  
2 **net community production from in-situ O<sub>2</sub>/Ar and satellite observation: A**  
3 **methodological study**

4 **S1. Supplementary Methods**

5 **S1.1 General Description**

6 The SOM methodology partitions a potentially large, high-dimensional dataset into a smaller  
7 number of representative clusters. In contrast with conventional cluster analysis, these SOM  
8 clusters, each of which is associated with a component called a node or neuron, become  
9 topologically ordered on a lower-dimensional, typically two-dimensional, lattice so that similar  
10 clusters are located close together in the lattice and dissimilar clusters are located farther apart.  
11 This topological ordering occurs through the use of a neighborhood function, which acts like a  
12 kernel density smoother among a neighborhood of neurons within this low-dimensional lattice.  
13 As a result, neighboring neurons within this lattice influence each other to produce smoothly  
14 varying clusters that represent the multi-dimensional distribution function of the data used to  
15 construct the SOM.

16 Our approach of determining predictor/predictand SOM clusters is quite similar to that of  
17 *Telszewski et al.* [2009] except for one main difference: we incorporate the predictand into the  
18 SOM analysis rather than labeling each neuron with an associated NCP value after the SOM has  
19 been trained. Thus we combine the first two steps of map generation from *Telszewski et al.*  
20 [2009] into a single step. We choose this alternative approach so that the neighborhood function,  
21 which smoothes the clusters in the data space, may operate on the NCP as well as the predictor  
22 data.

23 **S1.2 Cross-validations**

24 To determine a set of candidate predictor and parameter combinations, we first perform a set  
25 of cross-validation tests in the following manner. We identify 39 weeks in the ship track  
26 database that have at least five days of NCP data within a seven-day period and then divide these  
27 39 weeks into five validation segments (eight weeks each segment except one with seven

28 weeks). We next perform a five-fold cross-validation for many predictor/parameter  
29 combinations, whereby we train the SOM with all ship track data excluding the validation  
30 segments and evaluate the prediction of weekly mean NCP for the validation segments in five  
31 separate iterations. To minimize the possibility that the data in the validation and training  
32 samples are highly correlated and thus leading to over-confident NCP predictions, we add the  
33 condition that the data from any particular ship track cannot be split between training and  
34 validation samples. We calculate the MAE, RMSE, and MFE of the predicted NCP.

35 For the SOM parameter combinations we evaluate the following values for the number of  
36 rows and columns: 1-6, 8, 10, 12, 14, 18, and 24. We also vary the final neighborhood radius  
37 from zero to five. With 12 possible values for the number of rows and columns and six values  
38 for the final neighborhood radius, we test 864 possible SOM parameter combinations. In  
39 addition, we test all 63 possible predictor combinations to give a total of 54,432 cross-validation  
40 tests. We record the parameter combination with the minimum MAE, RMSE, and MFE for each  
41 of the 63 predictor combinations.

## 42 **S2. Interannual NCP variability**

43 To explore the potential use of our constructed dataset to study interannual NCP variability,  
44 we present snapshots of November NCP for 2003 and 2004 in Figures S1a and S1b. These  
45 results should be interpreted with caution because we have not yet assessed the uncertainty in  
46 interannual predictions. In both figures, two large patches of high NCP are seen over southwest  
47 Atlantic in the Brazil-Malvinas Confluence zone as well as in the region near southeast Australia  
48 and New Zealand, which are marked with blue squares in Figure S1. Our constructed dataset  
49 predicts variations between these two years in the two regions. The Australia-New Zealand  
50 patch (140°E–170°W, 35°S–46°S) exhibits a distinct southeastward extension in 2003 (Figure  
51 S1a), whereas it is zonally confined in 2004 (Figure S1b). Over the Brazil-Malvinas patch  
52 (65°W–45°W, 35°S–46°S), the area-averaged NCP decreases from 37 to 27  $\text{mmol C m}^{-2}\text{d}^{-1}$  from  
53 2003 to 2004. The November maps of POC (Figures S2a, b) and Chl (not shown) also show  
54 similar variations for the same years, which support the physical basis for these NCP changes.  
55 The pattern correlation between NCP and POC ( $\log_{10}(\text{Chl})$ ) are 0.48 (0.42) and 0.47 (0.39) for  
56 2003 and 2004, respectively.

57 These large-scale variations in biological productivity plausibly may relate to dominant  
58 modes of the ocean-atmosphere interaction and the associated atmospheric teleconnections, as  
59 well as ocean current variability. For example, possible contributors include the change from  
60 neutral ENSO to El Nino conditions between 2003 and 2004 [Yu *et al.*, 2012], and the  
61 pronounced southward shift of the Brazil Current front from the continental shelf observed in  
62 2003 [Goni *et al.*, 2011]. However, more in depth analysis of the mechanisms of variability is  
63 reserved for future studies.

64 One may question whether the constructed NCP dataset can capture intraseasonal and  
65 interannual variability, given the fairly weak relationship between daily NCP and POC/Chl in the  
66 ship track observations, as reported in the main text, the temporal correlation between daily NCP  
67 and POC/ $\log_{10}(\text{Chl})$  is only 0.20/0.23. Because the residence time of POC and NCP integration  
68 time are of similar magnitude, 1–2 weeks in the surface ocean, and POC is the dominant form of  
69 NCP in the Southern Ocean, the low correlation between POC and NCP on daily timescales  
70 suggests sub-weekly transient processes and/or measurement errors that weaken the POC/NCP  
71 relationship.

72 The weak correlation between NCP and Chl is similar to the value of 0.33 reported in Reuer  
73 *et al.* [2007], although Reuer *et al.* [2007] consider area averages in three discrete zones for each  
74 of 23 transits rather than discrete points along the ship tracks. However, a substantially  
75 improved correlation of 0.62 is achieved in Reuer *et al.* [2007] between the *in situ* NCP and  
76 NPP, calculated using the VGPM (Vertically Generalized Productivity Model) of Behrenfeld and  
77 Falkowski [1997] that accounts for additional predictors (e.g., Chl, SST, and PAR). Given that  
78 our SOM-based approach includes additional biogeochemical and physical properties, aside from  
79 Chl that is also incorporated in the VGPM NPP estimates of Reuer *et al.* [2007], that our results  
80 are constrained by *in situ* observations, and that we find good agreement with previously  
81 reported independent, *in situ* NCP measurements (Tables 3.2 and 3.3) through real-time  
82 comparisons, we expect that our reconstruction explains a larger fraction of NCP variance on  
83 intraseasonal and interannual timescales than indicated by the low POC and Chl correlations.  
84 Additional validation tests are required to assess the reliability of the predicted interannual and  
85 possibly intraseasonal NCP variability, and relation to plausible physical mechanisms.

86

87 **Reference**

88 Behrenfeld, M. J., and P. G. Falkowski (1997), Photosynthetic rates derived from satellite-based  
89 chlorophyll concentration, *Limnol. Oceanogr.*, *42*, 1-20.

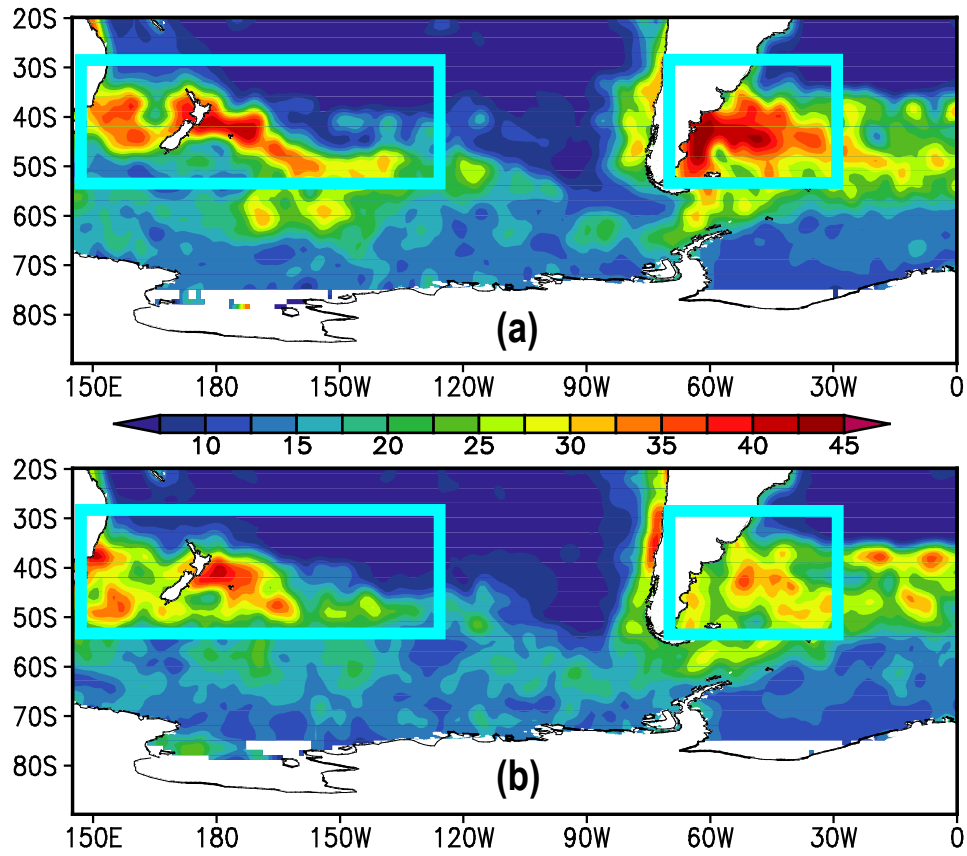
90 Goni, G.J., F. Bringas, and P.N. DiNezio (2011), Observed low frequency variability of the  
91 Brazil Current front, *J. Geophys. Res.*, *116*, doi:10.1029/2011JC007198.

92 Reuer, M. K., B. A. Barnett, M. L. Bender, P. G. Falkowski, and M. B. Hendricks (2007), New  
93 estimates of Southern Ocean biological production rates from O<sub>2</sub>/Ar ratios and the triple  
94 isotope composition of O<sub>2</sub>, *Deep-Sea Res., Part I*, *54*, 951-974.

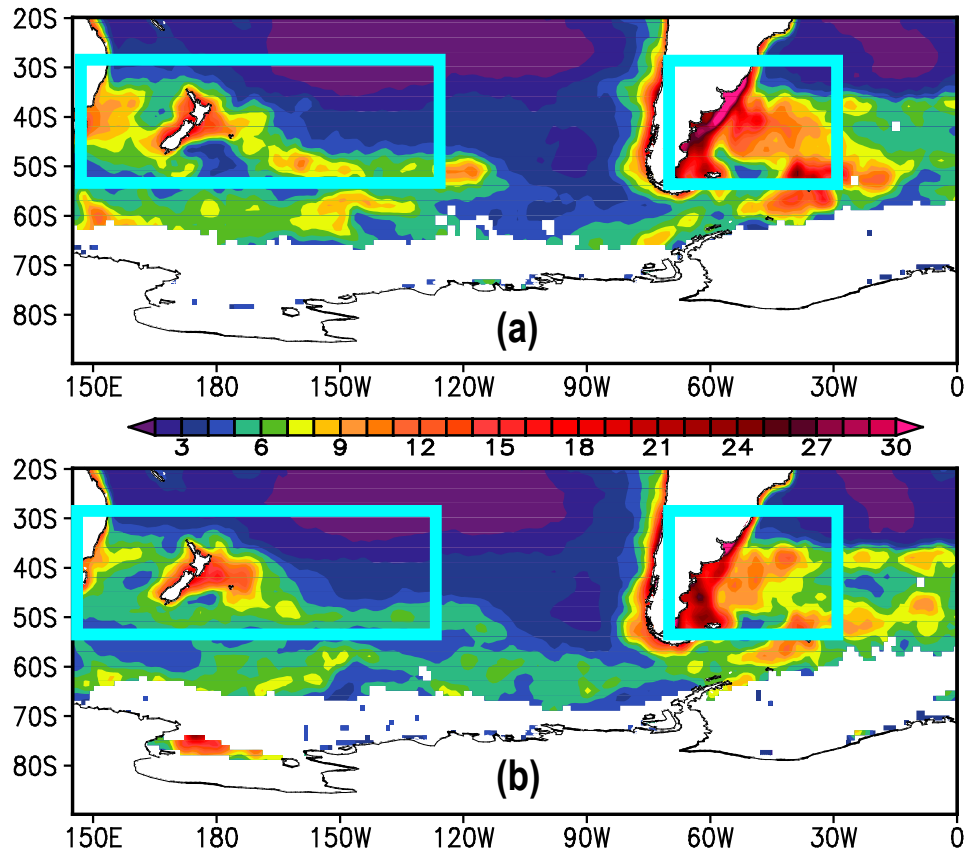
95 Telszewski, M., et al. (2009), Estimating the monthly pCO<sub>2</sub> distribution in the North Atlantic  
96 using a self-organizing neural network, *Biogeosciences*, *6*, 1405-1421, doi 10.5194/bg-6-  
97 1405-2009.

98 Yu, J.-Y., Y. Zou, S.T. Kim, and T. Lee (2012), The changing impact of El Niño on US winter  
99 temperatures, *Geophys. Res. Lett.*, *39*, doi:10.1029/2012GL052483.

100



100 **Figure S 1.** November NCP ( $\text{mmol C m}^{-2} \text{d}^{-1}$ ) for (a) 2003, and (b) 2004. The blue squares mark  
101 the two regions discussed in the supporting text.  
102



102 **Figure S 2** As in Figure S1 but for POC ( $\text{mmol C m}^{-3}$ ).

103